COBEM 2023 27TH INTERNATIONAL CONGRESS OF MECHANICAL ENGENEERING

ABCM Brazilian Society of Mechanical Sciences and Engineering
27th ABCM International Congress of Mechanical Engineering
December 04-08, 2023, Florianópolis-SC, Brazil

COB-2023-1448
CHARACTERIZATION AND EXPERIMENTAL ANALYSIS OF STRESS CORROSION CRACKING AND ITS INFLUENCE ON THE STRUCTURAL INTEGRITY AND MECHANICAL PROPERTIES OF THE MAGNESIUM ALLOY WE43

Geraldine Hincapie Diaz
Aeronautical Engineering Department / São Carlos School of Engineering / University of São Paulo - Av. João Dagnone, 1100 - Jardim Santa Angelina - São Carlos, SP, Brasil - 13563-120
ghincapied@usp.br

Carlos Alberto Della Rovere
Federal University of São Carlos / Rodovia Washington Luis, km 235 - São Carlos, SP, Brasil - 13565-905
rovere@ufscar.br

Marcelo Leite Ribeiro
Aeronautical Engineering Department / São Carlos School of Engineering / University of São Paulo - Av. João Dagnone, 1100 - Jardim Santa Angelina - São Carlos, SP, Brasil - 13563-120
malribei@usp.br

Abstract. *Magnesium alloys have been widely studied as biodegradable metals, due to their low density and fast dissolution properties, and are considered a good alternative for use as medical support implants, since their compatibility and degradation in the human body makes a second surgery unnecessary. However, magnesium alloys must maintain their mechanical integrity in the body during the healing period, and besides the low corrosion resistance in general, it is very susceptible to stress corrosion, which can cause premature and sudden fractures of the implant. This is one of the problems that hinder the use of this product, and it is crucial to analyze the behavior against this phenomenon in order to understand the effects of this occurrence on the mechanical properties and structural integrity of magnesium alloys. Thus, this work aims to characterize and experimentally analyze the effects of stress corrosion on WE43 alloy. To this end, constant load tests were conducted using a portable and adaptable device equipped with compression springs to apply tensile force. The tests were performed by immersing the specimens in Simulated Body Fluid (SBF) to simulate the corrosive environment, and two annealing conditions were employed to analyze the influence of the corrosive environment on the mechanical properties of the material. Based on the results, it was observed that the specimens annealed with a temperature of 400°C and a duration of 15 minutes exhibited a significant improvement in mechanical properties, particularly in ductility and corrosion resistance, compared to the samples annealed at 500°C for 15 minutes. The findings highlight the influence of heat treatment on the mechanical properties and corrosion resistance of magnesium alloys. Annealing treatments at specific temperatures and durations promote the formation of a protective oxide layer on the alloy surface, enhancing resistance to stress corrosion. The study concluded that the simultaneous effect of stress and the corrosive environment (stress corrosion) was the primary cause of the loss of mechanical properties in both annealing conditions of the WE43 alloy, while stress-independent corrosion contributed only marginally.*

Keywords: *Magnesium alloy, WE43, Stress Corrosion Cracking, Biodegradable materials.*

1. INTRODUCTION

Interest in magnesium-based implants has experienced exponential growth over the past 15 years. This is primarily due to the inherent characteristics of magnesium, such as its spontaneous and relatively rapid dissolution, making it an attractive option as a biodegradable and biocompatible metal (Mordike and Ebert (2001)). Additionally, magnesium plays a crucial role in human metabolism, serving as a source for numerous enzymes. As a result, unlike traditional implant materials like titanium and stainless steel, the degradation products of magnesium are non-toxic to the human body (Li *et al.* (2004); Staiger *et al.* (2006)). Numerous studies have reported that the magnesium ions released during degradation have a positive impact on tissue healing. Furthermore, any excess magnesium in the body is efficiently eliminated through urine excretion. These properties further enhance the appeal of magnesium-based implants for biomedical applications

(Saris *et al.* (2000); Choudhary and Raman (2012)).

The study of magnesium alloys in biomedicine has led to significant advancements, especially in cardiovascular devices like stents and temporary orthopedic devices that require structural integrity during the healing process Gastaldi *et al.* (2011). The prolonged presence of implants in the body can give rise to adverse health effects, as conventional materials eventually become incompatible, necessitating a secondary surgery for implant removal. This issue could be mitigated by implementing biodegradable devices (Esmaily *et al.* (2017); Choudhary and Raman (2012)).

The biodegradability of magnesium (Mg) alloys is closely tied to their corrosion behavior, which is influenced by various factors, including alloy composition, processing, surface finishing, corrosion environment, and load conditions. The corrosion process of Mg in neutral aqueous environments involves an electrochemical reaction with water, resulting in the formation of magnesium hydroxide and hydrogen gas. The overall corrosion reaction of Mg can be represented by Equation (1). However, in physiological environments with high chloride concentrations, this protective layer is susceptible to breakdown, as indicated by Equation (2), leading to further corrosion. (Gastaldi *et al.* (2011); Song and Atrens (2003)).

$$Mg + 2H_2O \rightarrow Mg(OH)_2 + H_2 \tag{1}$$

$$Mg(OH)_2 + 2Cl^- \rightarrow MgCl_2 \tag{2}$$

Magnesium and its alloys are susceptible to different corrosion mechanisms, including microgalvanic corrosion, localized pitting corrosion, stress corrosion cracking , and fatigue corrosion (Choudhary and Raman (2012)). Microgalvanic corrosion arises from the difference in electrochemical potential between the magnesium, acting as the anode, and secondary or impurity phases, which act as the cathode, resulting in highly localized corrosion. Pitting corrosion occurs when the protective passivation layer of the material breaks down upon exposure to aggressive physiological environments, especially those rich in chloride solutions. This type of corrosion begins as irregular pits that propagate laterally, eventually covering the entire surface. Stress corrosion cracking involves the interplay between the material, the environment, and applied stress. It can manifest as either intergranular or transgranular cracking, with the former associated with cracks forming and propagating due to localized corrosion defects, and the latter related to cracks arising from hydrogen embrittlement (Song and Atrens (2003)).

The specific mechanisms governing Stress Corrosion Cracking (SCC) in WE43 implants are influenced by various factors, including the implant's microstructure, the applied stress conditions, and the composition of the surrounding bodily fluid. For instance, implants with a larger grain size or a higher concentration of intermetallic precipitates are more prone to SCC. Furthermore, implants subjected to elevated levels of stress or exposed to chloride ions are at an increased risk of SCC (Winzer *et al.* (2005)). There are several key mechanisms involved in SCC:

- Anodic dissolution: It is the initial stage in all corrosion processes. It entails the oxidation of magnesium atoms on the implant's surface, resulting in the formation of magnesium ions. These ions dissolve in the surrounding body fluid. Concurrently, the released electrons from this process reduce hydrogen ions in the body fluid, generating hydrogen gas. The hydrogen gas can diffuse into the magnesium alloy, leading to hydrogen embrittlement (Winzer *et al.* (2005)).
- Hydrogen embrittlement: It occurs when hydrogen atoms diffuse into the metal and form hydrogen bubbles at grain boundaries. These hydrogen bubbles weaken the grain boundaries, making the metal more susceptible to cracking.
- Transgranular SCC: Takes place within the grains of the magnesium alloy. It begins with the formation of microcracks at grain boundaries or other microstructural defects. These microcracks then propagate through the grains under the combined influence of stress and corrosion (Abdalla *et al.* (2020)).
- Intergranular SCC: Intergranular SCC occurs along the grain boundaries of the magnesium alloy. It commences with the formation of a corrosion product at the grain boundaries. This corrosion product weakens the grain boundaries, rendering them susceptible to cracking (Abdalla *et al.* (2020)).

Studies of magnesium alloys have demonstrated that materials used as implants are not only subject to general corrosion mechanisms but also experience biomechanical stresses within the human body. These stresses include both compressive and tensile forces. For instance, the knee joint operates in a complex mechanical environment encompassing activities such as rotation, flexion, and extension. In this scenario, the highest tensile stress occurs in the anterior cruciate

ligament (ACL), measuring approximately 15 MPa (Gao *et al.* (2019)). Similarly, a hip implant during normal gait can endure loads of approximately four times the body weight. In contrast, a cardiovascular stent continuously faces cyclic loads due to the beating heart (Choudhary and Raman (2012)).

When a magnesium alloy sample is subjected to stress in the presence of a corrosive environment, such as body fluid or saline solutions that simulate human body conditions, stress application leads to the formation of micro-cracks on the sample's surface. These micro-cracks become preferential sites for localized corrosion and stress corrosion, as explained by Fairman and West (1965). During this process, magnesium ions dissolve in the corrosive environment, resulting in a reduction of the specimen's cross-sectional area and an increase in stress at the microcrack locations. Consequently, crack propagation accelerates, ultimately leading to specimen failure, even at stress levels below the material's yield strength, as observed by Winzer *et al.* (2005).

With the objective of addressing the limitations associated with magnesium alloys used as biodegradable materials, this study aims to experimentally analyze the impact of stress corrosion on the mechanical properties and corrosion rate of the material, under conditions that closely resemble those encountered within the human body.

2. MATERIALS AND METHODS

2.1 Sample

The magnesium alloy WE43MEO, manufactured by Meotec GmbH (Germany) and supplied by Fort Wayne Metals (USA), with the following chemical composition (wt. %) was used as material: Mg - bal, Y - 4.1, RE - 4.0, Zr - 0.5. The material was supplied in wire form, with a diameter of 0.88 mm.

2.2 Mechanical characterization tests

Annealing is a widely applied heat treatment process for various metals and alloys, including magnesium alloys like WE43. This treatment involves heating the material to a specific temperature and maintaining it at that level for a certain duration, followed by controlled cooling. Its purpose is to render the material more pliable, alleviate internal stresses, and enhance its ductility and toughness.

Regarding WE43, an annealing heat treatment holds the potential to reverse the strengthening effects of cold drawing and aging, rendering the material more ductile and less susceptible to cracking or failure under particular conditions. However, the precise outcomes of an annealing treatment on WE43's properties would hinge on the specific parameters employed, including temperature, duration, and cooling rate. After a comprehensive review of the literature and considering the best results achieved by various authors, it was decided to implement two heat treatments: one at 400°C for 15 minutes and another at 500°C for 15 minutes (Maier *et al.* (2015); Griebel *et al.* (2017); Mardina *et al.* (2023)).

Following the heat treatment, tensile tests were conducted to assess the mechanical properties of the magnesium alloy. An INSTRON universal testing machine was employed, and the tests were performed at a controlled speed of 1 mm/min. Each specimen possessed dimensions of D 0.88mm x 80mm and a useful length of 50mm, as illustrated in "Fig. 1".

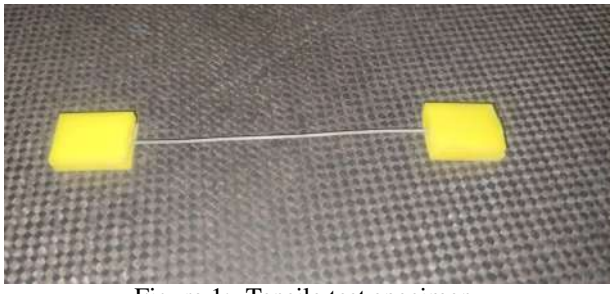

Figure 1: Tensile test specimen.

2.3 Stress corrosion testing

Stress corrsion tests are commonly conducted using constant load tests. In this type of test, the material's tensile strength is sustained until failure occurs at different fixed stress levels within a corrosive environment. The objective is to identify the stress limits and evaluate the time to failure, particularly when failure tends to be non-existent. In the case of the WE43 alloy, these tests are performed under the same conditions and in a corrosive environment.

For conducting stress corrosion experiments, a device based on the C test described by Choudhary and Raman (2012)

is used as a reference. This device is designed to generate tensile stress in the specimens. The device structure is made of a polymer, specifically polyacetal, chosen to minimize the risk of galvanic corrosion. Stainless steel guides are employed to ensure that the specimens are loaded purely in uniaxial tension ("Fig. 2").

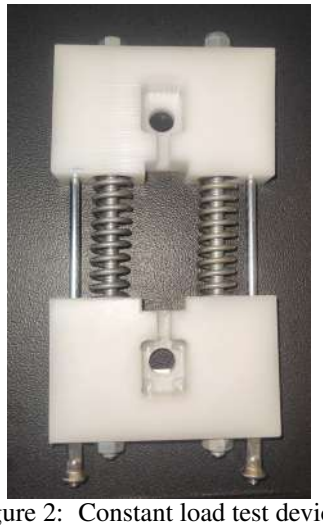

Figure 2: Constant load test device.

In the device, two calibrated compression springs are used to apply the load to the specimens. The springs are compressed to a defined length based on the desired load value. This is achieved by tightening two bolts that pass through the inner diameter of the springs, securing the specimen in place. To release the load from the springs onto the specimen, the screws are loosened. It is worth noting that the gradual elongation of the specimen in the solution has a minimal effect on the applied load, with a reduction of less than 1.1 N (1.8% of the lowest applied load) observed.

For immersion stress corrosion biodegradation tests, a conventional simulated body fluid (c-SBF) is used as the electrolyte, produced based on "Tab. 1". This choice is based on its widespread usage and its favorable ionic and pH stability for storage.

Table 1: Quantity of reagents for SBF preparation.

Reagent	**Purity (%)**	**Amount**
NaCL	>99,5	8,036g
NaHCO3	>99,5	0,352g
KCL	>99,5	0,225g
K2KPO4 * 3H2O	>99,0	0,230g
MgCl2*6H2O	>98,0	0,311g
1,0 M * HCL	-	40ml
CaCL2	>95,0	0,293g
Na2SO4	>99,0	0,072g
TRIS	>99,9	6,063g
1,0 M * HCL	-	0,2ml

(Oyane *et al.* (2003))

The specimens used in these tests, referred to as SPs, have a diameter of 0.88mm and a usable length ranging between 65mm and 69mm. To begin the testing process, it is necessary to prepare the specimens by subjecting them to chemical cleaning with 20% chromic acid. This step aims to remove surface oxides from the specimens. Following the cleaning process, the mass of each specimen should be measured and documented to enable identification. Subsequently, the SPs are assembled in the testing device.

After the immesion period, the specimens are removed from the corrosion electrolyte. They undergo cleaning once again, this time using 20% chromic acid, followed by rinsing with distilled water. This cleaning procedure ensures the removal of any corrosion products present on the surface of the SPs. Finally, the weight of each specimen is measured using a balance to determine the mass loss experienced during the degradation process.

3. RESULTS AND DISCUSSIONS

3.1 Mechanical characterization

Initially, a uniaxial tension test is performed to verify the mechanical properties of the material and validate the subjection method in the stress corrosion tester, because there may be slippage or excessive force concentrations at the ends where the SP specimen is subjected, to mitigate these issues, it is proposed to attach polymeric clamps or tabs to the SP specimens, as illustrated in "Fig. 3". "Figure 4" shows the stress-strain curve obtained from the tensile test conducted before and after two heat treatments.

Figure 3: Setting up the tensile test on the universal machine.

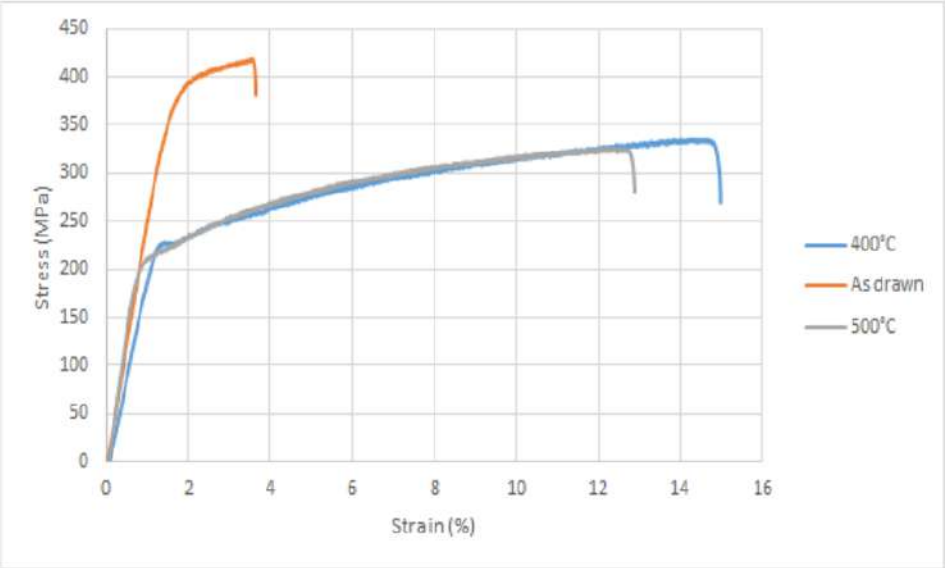

Figure 4: Average stress-strain curves from tensile testing of wire specimens, for both As drawn and Annealed conditions.

The "Figure 4" illustrates the influence of the annealing heat treatment on the stress-strain curve of WE43. It is evident that both annealing processes led to a substantial improvement in the alloy's ductility. Specifically, ductility increased from 3.3% to 12.8% and 15% strain. However, this enhancement in ductility was accompanied by a reduction in

the ultimate tensile strength, which experienced an approximately 32% decrease. The grey line on the graph represents the 500°C-15min annealing, demonstrating a slight decrease in both the ultimate tensile strength and yield strength, with a 2% lower strain compared to the 400°-15 annealing.

According with Mardina *et al.* (2023), annealing increases the grain size of the alloy. This can make the alloy less strong and more susceptible to creep, but it can also improve the alloy's toughness. Annealing can enhance the corrosion resistance of the alloy by relieving internal stresses and homogenizing the microstructure.

On the other hand, in a study referenced by Yang *et al.* (2019) and Mardina *et al.* (2023), it was observed that the annealing heat treatment leads to the following changes in the alloy: The hardness and strength of the alloy decrease. This phenomenon can be attributed to the lower dislocation density and the larger grain size. As the grain size increases, the number of grain boundaries, which act as obstacles to dislocation motion, decreases, resulting in reduced strength. However, the larger grain size and decreased dislocation density promote plastic deformation, allowing for improved plasticity and elongation before fracture (Wang *et al.* (2019)). This is particularly advantageous for this study as high deformability and resistance to cracking are required for applications involving the magnesium alloy (Choudhary *et al.* (2014)).

The results are consistent with those reported by Maier *et al.* (2015) and with the characterization by Saconi (2021). "Table 2" displays the material properties under the three different conditions.

Table 2: Average mechanical properties for both As drawn and Annealed wire specimens.

Thermal Condition	**UTS (MPa)**	**Yield Stress (MPa)**	**Elongation at break (%)**
As Drawn	420.4 ± 10.3	389.9 ± 10.2	3.50 ± 1.2
Annealed 400°C - 15min	356.7 ± 2.4	245.9 ± 8.5	15 ± 0.2
Annealed 500° - 15min	319,40 ± 2,6	292.74 ± 5.2	12,8 ± 2,2

4. Stress corrosion test

Tests were conducted with two different conditions while maintaining the assembly as depicted in the "Fig. 5". In the first condition, 5 specimens underwent annealing heat treatment at 400°C for 15 minutes. For the second condition, a heat treatment at 500°C for 15 minutes was performed to 5 specimens.

Figure 5: Experimental setup.

4.1 Stress corrosion testing - first condition

"Figure 6" illustrates two specimens immersed in the SBF (simulated body fluid) solution, and they are subjected to a constant load of 181.73MPa and 93.16MPa. These loads correspond to 80% and 40% of the yield strength of the magnesium alloy WE43, respectively. Both samples were simultaneously placed in the solution and underwent identical chemical cleaning and heat treatment procedures prior to testing.

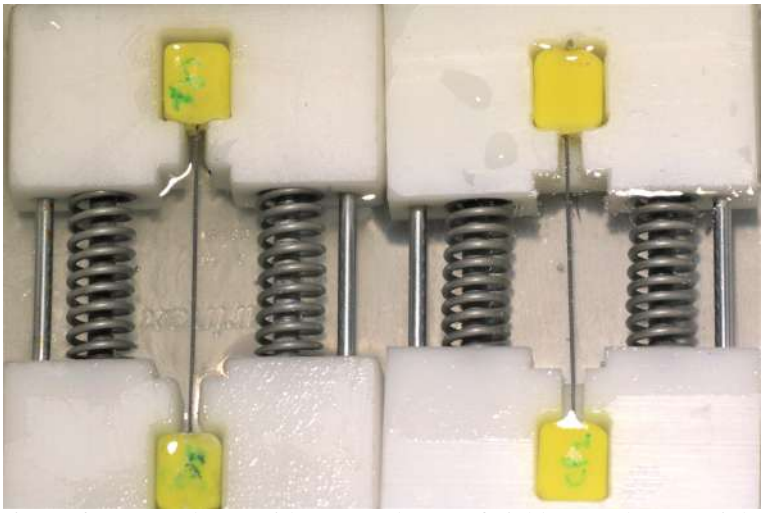

Figure 6: SP1 and SP2 with 40% and 80% of yield strength respectivly.

"Figure 7" both specimens, SP1 and SP2, experienced failure. SP1, subjected to a stress of 93.16MPa, ruptured after 149 hours of testing. On the other hand, SP2, which was subjected to a higher stress of 181.73MPa, ruptured after 64 hours of testing. "Table 3" provides the data and main results from the tested specimens.

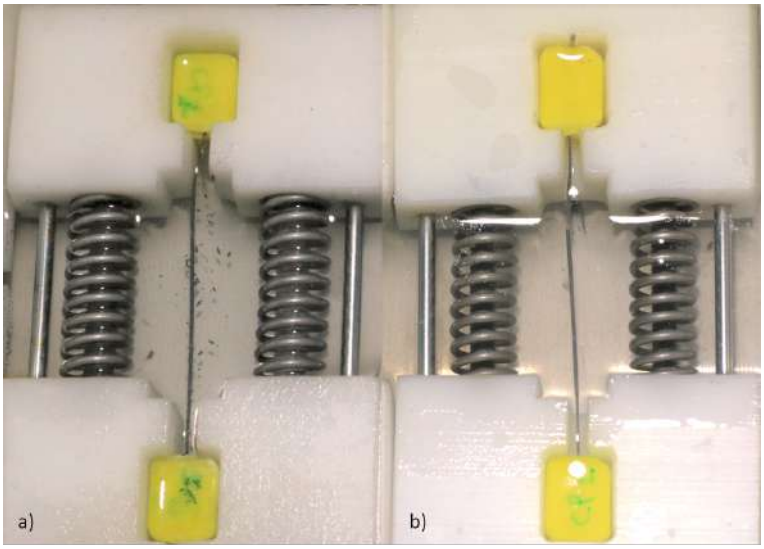

Figure 7: a)SP1 and b)SP2 failure.

Table 3: Summary of Stress Corrosion Test Results with Heat Treatment 400 - 15 min.

	CP1	CP2	CP3
Lo (mm)	69	65	67
Lo spring (mm)	45,5	41	43
F(N)	55,898	109,04	78,4532
Stress (Mpa)	93,16	181,73	130,755
% Yield Stress	40	80	60
Wo (g)	4,2339	4,0123	0,1213
Wf(g)	4,1615	3,9804	0,0723
Time to failure (h)	149	64	100

4.2 Stress corrosion test - second condition

The tests were repeated for the second group of specimens, and in this case, they underwent annealing heat treatment at 500°C for 15 minutes. Similarly, 5 specimens were immersed in the SBF solution until failure, with stresses ranging between 40% and 70% of the material's yield strength. The "Figure 8" displays two specimens, SP1 with a stress of 83.85MPa and SP2 with a stress of 102.716MPa.

Additionally, the "Figure 9" presents the specimens at the time of fracture, with SP1 (left) breaking after 53 hours of testing, SP2 (right) after 51 hours, and SP3 after 40 hours of testing. The "Table 4" provides a summary of the main parameters used in the tests and the results obtained, including failure time and final mass.

Figure 8: SP1 and SP2 with 40% and 50% of yield limit respectivly.

Figure 9: SP1 and SP2 failure.

Based on the results obtained from the two test conditions on the material, two graphs have been generated to analyze the behavior of the material after the stress corrosion cracking (SCC) test and to compare the results based on the two annealing conditions. "Figure 10" presents the results of the stress corrosion to fracture tests. The applied stress is calculated as the ratio between the applied load and the cross-sectional area of the original specimen. This graph allows for the determination of the failure time based on the applied load and estimation of the threshold stress σ_{th}, which represents the stress level below which SCC failure does not occur. Furthermore, it aims to identify the influence of heat treatment on the material's behavior (Dietzel *et al.* (2011)).

In both cases, it is observed that increasing the applied stress leads to a significant reduction in the time to fracture

Table 4: Summary of Stress Corrosion Test Results with Heat Treatment 500 - 15 min.

	CP1	CP2	CP3
Lo (mm)	59	58	57
Lo spring (mm)	40 -39,5	38,5-39	37 -36,5
F(N)	50,31	61,63	84,53
Stress (Mpa)	83,85	102,716	140,88
% Yield Stress	40	50	60
Wo (g)	4,1162	3,7572	4,1282
Wf(g)	4,0845	3,7259	3,9991
Time to failure (h)	51	53	40

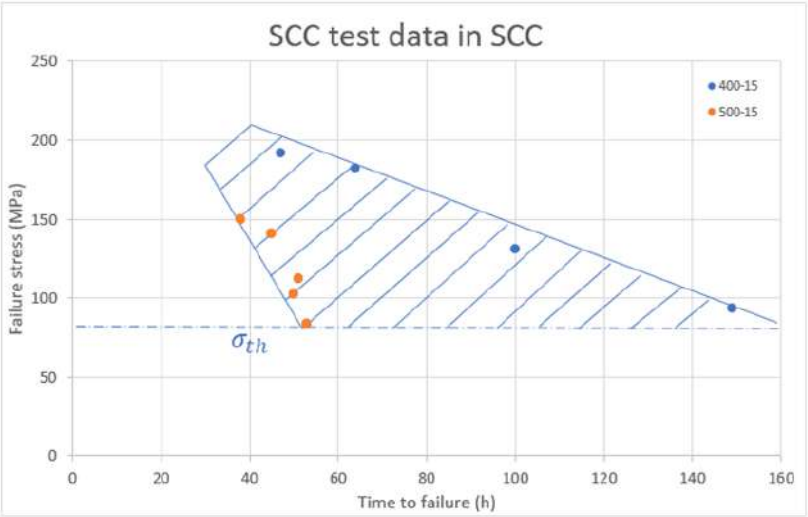

Figure 10: Time to failure and applied stress ratio obtained in a constant load CL test

of the specimens. However, in the tests with the first condition (blue), there is a notable halving of the time to fracture when the stress is increased from 90 MPa to 180 MPa. In the test with the second condition (orange), the time to fracture exhibits less variability compared to the first condition. Nevertheless, this represents a disadvantage compared to the specimens with the first condition, specifically those annealed at 400°C for 15 minutes. For instance, at a stress level of approximately 100 MPa, the 400°C-15min annealed specimens reach material rupture in 149 hours, whereas the 500°C-15min annealed specimens reach rupture in only 51 hours.

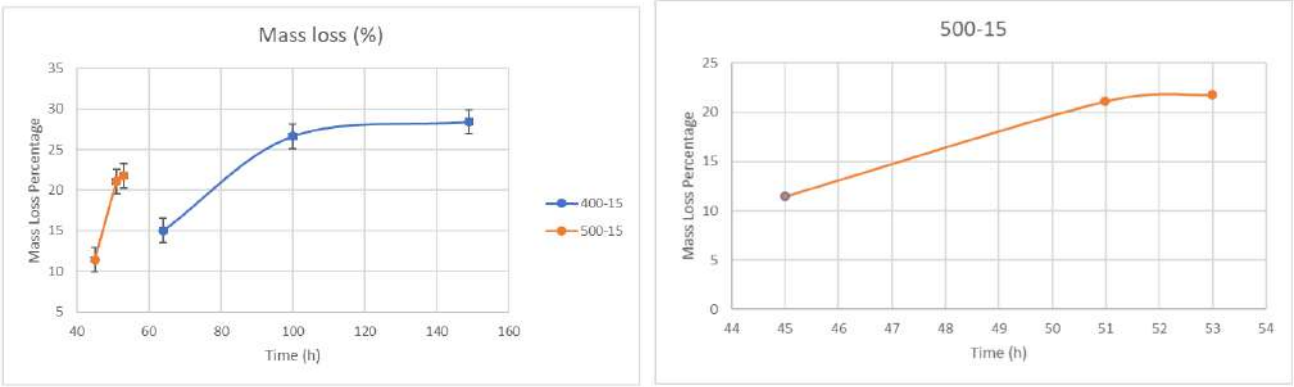

(a) Annealing 400-15. (b) Annealing 500-15.

Figure 11: Mass loss percentage and time to failure ratio

The mass loss results from the stress corrosion tests for both heat treatment conditions are depicted in “Fig. 11”. In both conditions, it is evident that the specimens experience a significant mass loss in the initial hours of the test. However, there

is a noticeable difference between the two sets of specimens. Those annealed with the 400°-15min condition managed to maintain their structural integrity for up to 149 hours under a stress level of 40% of the yield stress, resulting in a mass loss of 28.40%. Conversely, for the 500°-15min condition and the same stress percentage, an average mass loss of 21% was observed within a period of 53 hours.

This disparity can be attributed to the heat treatment process, which may promote the formation of a protective oxide layer on the surface of the alloy, thereby enhancing its resistance to corrosion in various environments. Thus, it is evident that the 400°-15min annealing condition not only positively influences corrosion resistance but also improves the alloy's ductility.

5. Conclusions

In the constant load SCC (Stress corrosion cracking) experiments, fractures were observed to occur below the yield strength in all tested SPs (specimens). The loads applied ranged between 40% and 80% of the yield strength. For the SPc specimens annealed at 400°-15min, the fractures occurred within a time range of 64 to 149 hours. Conversely, for the SPs with the 500°-15min annealing condition, fractures occurred between 38 hours with a load of 70% of the yield strength and 53 hours with a load of 40% of the yield strength.

Visible signs of corrosion, such as pitting and the formation of a coarse oxide layer on the material surface, were observed in all fractured SPs. The occurrence of fractures below the yield strength in all tested conditions indicates the presence of the SCC phenomenon.

6. REFERENCES

Abdalla, M., Joplin, A., Elahinia, M. and Ibrahim, H., 2020. "Corrosion modeling of magnesium and its alloys for biomedical applications: Review". *Corrosion and Materials Degradation*, Vol. 1, No. 2, pp. 219–248. ISSN 2624-5558. doi:10.3390/cmd1020011. URL https://www.mdpi.com/2624-5558/1/2/11.

Choudhary, L. and Raman, R.S., 2012. "Magnesium alloys as body implants: Fracture mechanism under dynamic and static loadings in a physiological environment". *Acta Biomaterialia*, Vol. 8, No. 2, pp. 916–923. ISSN 1742-7061. doi:https://doi.org/10.1016/j.actbio.2011.10.031. URL https://www.sciencedirect.com/science/article/pii/S174270611100482X.

Choudhary, L., Singh Raman, R., Hofstetter, J. and Uggowitzer, P.J., 2014. "In-vitro characterization of stress corrosion cracking of aluminium-free magnesium alloys for temporary bio-implant applications". *Materials Science and Engineering: C*, Vol. 42, pp. 629–636. ISSN 0928-4931. doi:https://doi.org/10.1016/j.msec.2014.06.018. URL https://www.sciencedirect.com/science/article/pii/S0928493114003804.

Dietzel, W., Srinivasan, P.B. and Atrens, A., 2011. "Testing and evaluation methods for stress corrosion cracking (scc) in metals". In *Stress Corrosion Cracking*, Elsevier, pp. 133–166.

Esmaily, M., Svensson, J., Fajardo, S., Birbilis, N., Frankel, G., Virtanen, S., Arrabal, R., Thomas, S. and Johansson, L., 2017. "Fundamentals and advances in magnesium alloy corrosion". *Progress in Materials Science*, Vol. 89, pp. 92–193. ISSN 0079-6425. doi:https://doi.org/10.1016/j.pmatsci.2017.04.011. URL https://www.sciencedirect.com/science/article/pii/S0079642517300506.

Fairman, L. and West, J.M., 1965. "Stress corrosion cracking of a magnesium aluminium alloy". *Corrosion Science*, Vol. 5, No. 10, pp. 711–716.

Gao, Y., Wang, L., Li, L., Gu, X., Zhang, K., Xia, J. and Fan, Y., 2019. "Effect of stress on corrosion of high-purity magnesium in vitro and in vivo". *Acta Biomaterialia*, Vol. 83, pp. 477–486. ISSN 1742-7061. doi:https://doi.org/10.1016/j.actbio.2018.11.019. URL https://www.sciencedirect.com/science/article/pii/S1742706118306731.

Gastaldi, D., Sassi, V., Petrini, L., Vedani, M., Trasatti, S. and Migliavacca, F., 2011. "Continuum damage model for bioresorbable magnesium alloy devices—application to coronary stents". *Journal of the mechanical behavior of biomedical materials*, Vol. 4, No. 3, pp. 352–365.

Griebel, A., Schaffer, J., Hopkins, T., Alghalayini, A., Mkorombindo, T., Ojo, K., Xu, Z., Little, K. and Pixley, S., 2017. "An in vitro and in vivo characterization of fine we43b magnesium wire with varied thermomechanical processing conditions". *Journal of Biomedical Materials Research Part B: Applied Biomaterials*, Vol. 106. doi:10.1002/jbm.b.34008.

Li, L., Gao, J. and Wang, Y., 2004. "Evaluation of cyto-toxicity and corrosion behavior of alkali-heat-treated magnesium in simulated body fluid". *Surface and Coatings Technology*, Vol. 185, No. 1, pp. 92–98. ISSN 0257-8972. doi:https://doi.org/10.1016/j.surfcoat.2004.01.004. URL https://www.sciencedirect.com/science/article/pii/S0257897204000258.

Maier, P., Griebel, A., Scheffler, O. and Schaffer, J., 2015. "Remaining strength of cold drawn and aged we43 wires after corrosion". *European cells materials*, Vol. 30, p. 47.

Mardina, Z., Venezuela, J., Sjafrizal, T., Shi, Z., Dargusch, M.S. and Atrens, A., 2023. "The influence of strain rate and annealing heat treatments on the corrosion and mechanical properties of we43 and zn7ag biodegradable wires for application in soft tissue reconstructions". *Materials Today Communications*, Vol. 35, p. 105809. ISSN 2352-4928. doi:https://doi.org/10.1016/j.mtcomm.2023.105809. URL https://www.sciencedirect.com/science/article/pii/S2352492823005007.

Mordike, B. and Ebert, T., 2001. "Magnesium: properties—applications—potential". *Materials Science and Engineering: A*, Vol. 302, No. 1, pp. 37–45.

Oyane, A., Kim, H.M., Furuya, T., Kokubo, T., Miyazaki, T. and Nakamura, T., 2003. "Preparation and assessment of revised simulated body fluids". *Journal of Biomedical Materials Research Part A*, Vol. 65A, No. 2, pp. 188–195. doi:https://doi.org/10.1002/jbm.a.10482. URL https://onlinelibrary.wiley.com/doi/abs/10.1002/jbm.a.10482.

Saconi, F., 2021. *Caracterização experimental e modelagem numérica do efeito da corrosão simulada nas propriedades mecânicas da liga de magnésio biodegradável WE43 para aplicações ortopédicas*. Ph.D. thesis, Universidade de São Paulo.

Saris, N.E.L., Mervaala, E., Karppanen, H., Khawaja, J.A. and Lewenstam, A., 2000. "Magnesium: An update on physiological, clinical and analytical aspects". *Clinica Chimica Acta*, Vol. 294, No. 1, pp. 1–26. ISSN 0009-8981. doi:https://doi.org/10.1016/S0009-8981(99)00258-2. URL https://www.sciencedirect.com/science/article/pii/S0009898199002582.

Song, G. and Atrens, A., 2003. "Understanding magnesium corrosion—a framework for improved alloy performance". *Advanced engineering materials*, Vol. 5, No. 12, pp. 837–858.

Staiger, M.P., Pietak, A.M., Huadmai, J. and Dias, G., 2006. "Magnesium and its al-

loys as orthopedic biomaterials: A review". *Biomaterials*, Vol. 27, No. 9, pp. 1728–1734. ISSN 0142-9612. doi:https://doi.org/10.1016/j.biomaterials.2005.10.003. URL https://www.sciencedirect.com/science/article/pii/S0142961205009014.

Wang, C., Yu, Z., Cui, Y., Yu, S., Ma, X. and Liu, H., 2019. "Effect of hot rotary swaging and subsequent annealing on microstructure and mechanical properties of magnesium alloy we43". *Metal Science and Heat Treatment*, Vol. 60, pp. 777–782.

Winzer, N., Atrens, A., Song, G., Ghali, E., Dietzel, W., Kainer, K.U., Hort, N. and Blawert, C., 2005. "A critical review of the stress corrosion cracking (scc) of magnesium alloys". *Advanced Engineering Materials*, Vol. 7, No. 8, pp. 659–693.

Yang, S.j., Li, Y.d., Dong, P.y., Li, J.m., Cao, C. and Ma, Y., 2019. "Effect of annealing process on the microstructures and mechanical properties of az31b/a356 composite plate fabricated by cast rolling". *Materials Research*, Vol. 22, No. 4, p. e20190001. ISSN 1516-1439. doi:10.1590/1980-5373-MR-2019-0001. URL https://doi.org/10.1590/1980-5373-MR-2019-0001.

7. RESPONSIBILITY NOTICE

The authors is are solely responsible for the printed material included in this paper.